Positive effects of cell-free porous PLGA implants and early loading exercise on hyaline cartilage regeneration in rabbits

Nai-Jen Chang [a,*], Chih-Chan Lin [b], Ming-You Shie [c], Ming-Long Yeh [d], Chien-Feng Li [e], Peir-In Liang [f], Kuan-Wei Lee [a], Pei-Hsun Shen [a], Chih-Jou Chu [a]

[a] Department of Sports Medicine, Kaohsiung Medical University, 100 Shih-Chuan 1st Rd., Kaohsiung City 807, Taiwan
[b] Laboratory Animal Center, Department of Medical Research, Chi-Mei Medical Center, 901 Zhonghua Rd., Yongkang Dist., Tainan City 701, Taiwan
[c] 3D Printing Medical Research Center, China Medical University Hospital, 2 Yude Rd., North Dist., Taichung City 404, Taiwan
[d] Department of Biomedical Engineering, National Cheng Kung University, 1 University Rd., Tainan City 701, Taiwan
[e] Division of Clinical Pathology, Department of Pathology, Chi-Mei Medical Center, 901 Zhonghua Rd., Yongkang Dist., Tainan City 701, Taiwan
[f] Department of Pathology, Kaohsiung Medical University Hospital, 100 Shih-Chuan 1st Rd., Kaohsiung City 807, Taiwan

ARTICLE INFO

ABSTRACT

The regeneration of hyaline cartilage remains clinically challenging. Here, we evaluated the therapeutic effects of using cell-free porous poly(lactic-co-glycolic acid) (PLGA) graft implants (PGIs) along with early loading exercise to repair a full-thickness osteochondral defect. Rabbits were randomly allocated to a treadmill exercise (TRE) group or a sedentary (SED) group and were prepared as either a PGI model or an empty defect (ED) model. TRE was performed as a short-term loading exercise; SED was physical inactivity in a free cage. The knees were evaluated at 6 and 12 weeks after surgery. At the end of testing, none of the knees developed synovitis, formed osteophytes, or became infected. Macroscopically, the PGI-TRE group regenerated a smooth articular surface, with transparent new hyaline-like tissue soundly integrated with the neighboring cartilage, but the other groups remained distinct at the margins with fibrous or opaque tissues. In a micro-CT analysis, the synthesized bone volume/tissue volume (BV/TV) was significantly higher in the PGI-TRE group, which also had integrating architecture in the regeneration site. The thickness of the trabecular (subchondral) bone was improved in all groups from 6 to 12 weeks. Histologically, remarkable differences in the cartilage regeneration were visible. At week 6, compared with SED groups, the TRE groups manifested modest inflammatory cells with pro-inflammatory cytokines (i.e., TNF-α and IL-6), improved collagen alignment and higher glycosaminoglycan (GAG) content, particularly in the PGI-TRE group. At week 12, the PGI-TRE group had the best regeneration outcomes, showing the formation of hyaline-like cartilage, the development of columnar rounded chondrocytes that expressed enriched levels of collagen type II and GAG, and functionalized trabecular bone with osteocytes. In summary, the combination of implanting cell-free PLGA and performing an early loading exercise can significantly promote the full-thickness osteochondral regeneration in rabbit knee joint models.

Statement of significance

Promoting effective hyaline cartilage regeneration rather than fibrocartilage scar tissue remains clinically challenging. To address the obstacle, we fabricated a spongy cell-free PLGA scaffold, and designed a reasonable exercise program to generate combined therapeutic effects. First, the implanting scaffold generates an affordable mechanical structure to bear the loading forces and bridge with the host to offer a space in the full-thickness osteochondral regeneration in rabbit knee joint. After implantation, rabbits were performed by an early treadmill exercise 15 min/day, 5 days/week for 2 weeks that directly exerts in situ endogenous growth factor and anti-inflammatory effects in the reparative site. The advanced therapeutic strategy showed that neo-hyaline cartilage formation with enriched collagen type II, higher glycosaminoglycan, integrating subchondral bone formation and modest inflammation.

© 2015 Acta Materialia Inc. Published by Elsevier Ltd. All rights reserved.

* Corresponding author. Tel.: +886 7 3121101x2646/625; fax: +886 7 3138359.
  E-mail address: njchang@kmu.edu.tw (N.-J. Chang).

1. Introduction

The status of articular cartilage is affected by multiple intrinsic and extrinsic factors [1,2]. Intrinsic factors include the composition and extracellular matrix (ECM) of the articular cartilage. Extrinsic factors include the loading and inflammatory stresses applied to the joint. Upon prolonged imbalanced homeostasis, the cartilage undergoes decreased ECM deposition, which eventually leads to irreversible cartilage lesions [3]. Currently, clinical interventional strategies for cartilage repair include arthroscopic resurfacing, bone marrow stimulation techniques (e.g., subchondral drilling), autologous chondrocyte implantation (ACI), and osteochondral transplantation. However, the main limitation of cartilage treatment options is the inability of traditional medicine to promote effective hyaline cartilage regeneration in the presence of regenerated fibrocartilage scar tissue, which hinders joint motion and leads to progressive degeneration [4].

The metabolic supply of articular cartilage depends on synovial fluid in joint motion rather than on blood vessels [5]. Therefore, control of a suitable microenvironment that includes the regulation of the synthetic (anabolic) and resorptive (catabolic) cytokines of the chondrocytes plays a critical role in facilitating the healing process for cartilage repair [6]. This microenvironment can be manipulated both (1) by implanting 3D grafts that provide a biologically compatible structure for cell adhesion, proliferation, and tissue development in the repair regions [7] and (2) by in-situ mechanical stimuli generated from joint motion [8].

With regard to implanting grafts, a poly(lactide-co-glycolide) (PLGA) implant can be porous, biocompatible and biodegradable and have superior mechanical properties, which are manipulated based on pore size and porosity in in vitro studies [9,10]. This implant creates a provisional matrix for new tissue regeneration in osteochondral defects in knee joints [11,12]. Furthermore, PLGA has been extensively adopted as a biomaterial in FDA-approved medical devices, in pre-clinical trials [13–17] and in clinical orthopedic applications [18].

Appropriate mechanical stimuli (e.g., application of bioreactors or physiotherapy exercises) not only provide metabolic transportation in cell growth but also directly affect the development of the hyaline cartilage [19]. Currently, enormous bioreactor systems that provide mechanobiological activation to cells have been used extensively to upregulate cell growth and ECM production [10,20]. However, these systems have been limited to partly mimicking physiological conditions in the joint microenvironment. Continuous passive motion (CPM), a non-weight-bearing therapy, has been reported to reduce joint swelling and the inflammatory response [8,21–23]. However, the formation of fibrocartilage scar tissue develops predominately in the defects, likely because joint motion without normal loading does not maintain normal articular cartilage [24,25]. Therefore, loading the joint is highly important for retaining the biophysiological and functional properties of the original articular cartilage [24,26]. Early loading exercises have been reported to reduce joint inflammation and to facilitate articular cartilage regeneration [26–28]. The fundamental principle of exercise lies in the physical facilitation of synovial fluid, which directly nourishes articular cartilage, with improved metabolic and nutritional transportation through loading and unloading forces during loading movement [29]. To date, pre-clinical trials in cartilage regeneration have mostly utilized a sedentary (SED) model [30,31], which corresponds to free cage activity for animals, with no postsurgical exercise. In addition, the effect of applying treadmill exercise on cartilage in an animal model has been studied only in either intact cartilage [27,32–35] or empty defect (ED) models [26,36–38]. However, no previous study has evaluated the therapeutic effect of scaffolding grafts combined with early loading exercise for osteochondral regeneration.

Therefore, we hypothesized that an engineered cell-free porous PLGA graft could provide a mechanostructural cue to stimulate cell adhesion and proliferation and tissue regeneration. Concurrently, loading exercise aids a biophysicochemical cue and exerts anti-inflammatory effects in the knee joint, thereby inducing the neighboring stem cells to self-renew and benefiting chondrogenesis and osteogenesis, thereby achieving the repair of osteochondral defects in the rabbit knee joint model.

2. Materials and methods

2.1. Porous PLGA grafts

Porous PLGA (lactide/glycolide ratio of 85/15, molecular weight 50 to 75 kDa) (Sigma, St. Louis, MO) grafts were fabricated using a solvent casting and particulate leaching technique, modified from our previously described method [25]. In brief, 5 ml of 20% w/v PLGA chloroform solution was mixed with 9 g sodium chloride (NaCl) particles of 300 to 500 μm in diameter, yielding a 90% (w/v) solution that was cast into a multi-hole cylinder mold 3 mm in diameter and 3 mm in height and lyophilized for 1 day to generate PLGA grafts. The grafts were soaked in deionized water to dissolve the NaCl porogens and then made into 3D sponge grafts (Fig. 1A). The characteristics of the porous PLGA grafts included a porosity above 90% and a controllable 300–500 μm pore size with interconnecting pores. Additionally, the fabricated PLGA grafts had a compressive tangent modulus of 0.65 MPa, as measured by a material testing system (LRX5K, Lloyd Instruments, U.K.) that is suitable for osteochondral defects in rabbits [11].

2.2. Surgical grafting procedure

The Animal Care and Use Committee of Kaohsiung Medical University approved all surgical animal experiments and aseptic procedures. An osteochondral defect in the rabbit knee joint model was established. In brief, a total of thirty 4-to-5-month-old New Zealand white male rabbits weighing 2–3 kg were utilized in this study, providing 56 knees for the experimental groups and 4 knees for the sham group. Prior to the experimental surgery, rabbits underwent anesthesia through the induction of a subcutaneous injection of Zoletil 50 (25 mg/kg) (Virbac, France). Subsequently, general anesthesia was maintained through automatic ventilator administration of a mixture of 2% isoflurane and oxygen (Panion & BF Biotech Inc., Taiwan). Under general anesthesia, bilateral legs were shaved, brushed, and disinfected. The status of the anesthesia was carefully confirmed via the pupillary reflexes. Subsequently, the knee was opened via an anteromedial parapatellar longitudinal incision to the joint capsule, followed by patellar dislocation laterally. The knee joint was flexed to expose the femoral trochlea. To hinder spontaneous recovery in the rabbit, a critical full-thickness osteochondral defect of 3 mm in diameter and 3 mm in depth was drilled on the femoral trochlear groove. To eliminate any possible heat effect that might lead to host cartilage damage, the joint was simultaneously flushed with sterile saline (0.9% NaCl) during drilling. Following the flush, cartilaginous and osseous debris were also removed from the defect.

Next, the rabbits were allocated randomly to the ED and PLGA graft implant (PGI) groups. In the PGI group, a previously sterilized PLGA graft, treated with 75% ethanol and then washed ten times with sterilized PBS, was placed in the defect region by press-fit fixation and subsequently irrigated with saline and repositioned in the patellar position, followed by wound closure. The joint
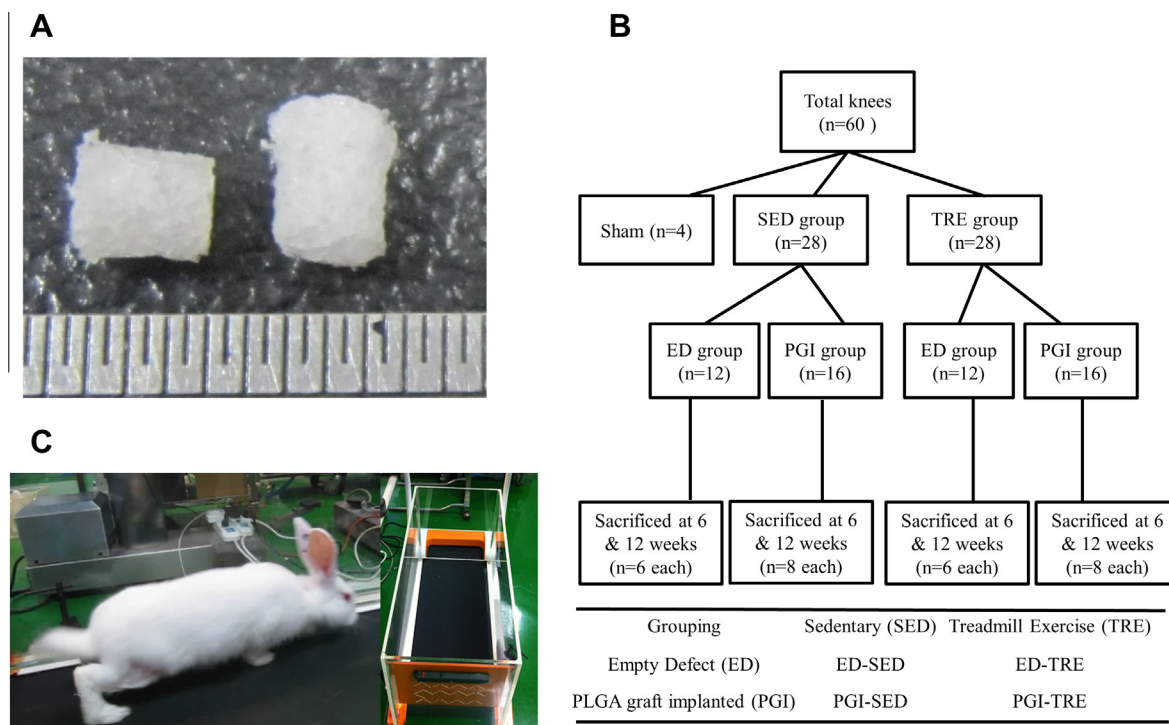
Fig. 1. (A) PLGA sponge grafts. (B) A schematic diagram of the animal grouping and the abbreviations of group names. (C) In the TRE group, the rabbits were subjected to exercise in a custom-designed treadmill with an electrical stimulation system.

capsule was repaired using 3–0 absorbable Vicryl sutures. The subcutaneous tissues and skin wound were closed using 3–0 nylon sutures. Moreover, in the sham group, the rabbits' knees were not drilled to create defects; the knees were only exposed and then sutured as described above. Each rabbit was individually housed in a 50 cm length by 40 cm width by 35 cm height stainless-steel cage. Antibiotic (25 mg/kg, Enrofloxacin) and analgesic (Ketoprofen) (Yung Shin Pharm., Taiwan) administration was performed for 3 days after surgery. The skin wounds were dressed with povidone iodine for 7 days. In addition, an animal collar (BUSTER, Denmark) was temporarily applied to prevent suture failure. Animal weights were recorded weekly throughout the experiment.

2.3. Animal grouping

The animal grouping and study design are shown in Fig. 1B. With or without the implantation of grafts, the rabbits were distributed into two exercise schemes as follows: (I) in the SED group, the rabbits were kept in their cages for free activity without any further exercise program until sacrifice; (II) in the TRE group, the rabbits were treated with early loading exercise 4 weeks post-surgery for a period of 2 weeks. All exercise periods were aided by a physical therapist (NJ Chang) and a veterinarian (CC Lin), both of whom observed the rabbits' stress responses. All rabbits were observed for body weight, eating and drinking, urination, wound healing, and functional activity after surgery. The rabbits were sacrificed at 6 and 12 weeks after surgery via intravenous injection of 120 mg/kg pentobarbital (Vortech Pharmaceutical, Dearborn, MI).

2.4. Exercise prescriptions

In the TRE group, the rabbits were subjected to exercise in a custom-designed treadmill with an electrical stimulation system (Fig. 1C). The dimensions of the walking surface were 34 × 96.5 cm. The treadmill was built with a fitted, transparent

acrylic enclosure (50 cm height × 100 cm long × 1 cm thick) that prevented the rabbits from jumping off of the treadmill surface. Initially, the rabbits were allowed to familiarize themselves with exercise on the treadmill five times in one week (at the lowest speed, 0.8 km/hr) for 10 min each time prior to receiving the operation. Four weeks post-surgery, the exercise treatment was initiated. The exercise intensity was adjusted to 1.0 km/hr, which Meng has identified as a mild to moderate exercise dosage for rabbits [39]. The timing of the exercise treatment at 4 weeks after the operation was performed as in previous studies [26,36]. It was suggested that exercise too early would damage the repairing tissue, whereas exercise too late might have an insignificantly beneficial impact on cartilage repair [26,40,41]. In this study, the rabbits were treated with exercise with a regime of warm-up, exercise, and cool-down for a total of 15 min/day, 5 days/week for 2 sequential weeks, whenever possible. During the exercise regime, the rabbits' temperatures were discreetly measured using a noncontact infrared thermometer (with an accuracy of 0.3 °C and a measurement time of less than 0.5 s) (TAISHENG, Taiwan) on the medial aspect of the base of the pinna, as rabbits regulate body temperature via their ears [42]. Thus, the heat regulation of a rabbit can be monitored before and after exercise as a vital sign indicator corresponding to exercise tolerance. Temperatures were measured in triplicate and averaged. The room temperature was set at 24 °C during all experimental measurements.

2.5. Gross appearance and macroscopic scores

After postsurgical euthanasia at week 6 (SED groups: 6 knees; TRE groups: 8 knees; sham: 4 knees) and week 12 (SED groups: 6 knees; TRE groups: 8 knees), the macroscopic scores of the regenerating tissue were blindly scored by two medical investigators in accordance with our previously reported scoring system [25]. The macroscopic appearance of each osteochondral defect on the femoral trochlear groove was assessed for coverage, tissue color,

and surface condition. The maximum total score was 12 points (Supplemental data 1). In this study, none of the SED or TRE knees developed synovitis, formed osteophytes, or became infected at either 6 or 12 weeks after surgery (Supplemental data 2A). The PGI-TRE group regenerated a smooth articular surface, with transparent new hyaline-like tissue soundly integrated with the neighboring cartilage, but the other groups remained distinct at the margins, showing fibrous or opaque tissues (Supplemental data 2A). Furthermore, the PGI-TRE group had significantly higher total macroscopic scores than the other groups (Supplemental data 2B). Interestingly, unlike in our previous study [25], we observed a variation in the macroscopic scores for the femoral medial condyle and femoral trochlear groove between groups, perhaps dependent on the defect location, including different healing remodeling patterns corresponding to the volume ratios of the newly formed bone.

2.6. μ-CT evaluations

To evaluate the qualitative and quantitative measurements of bone regeneration in the defects, a high-resolution μ-CT (SkyScan 1076; Kontich, Belgium) was adopted to scan the femoral trochlear groove in the ED and PGI groups. The SED (24 knees), TRE (32 knees) and sham (4 knees) groups were analyzed at the evaluation time point. The femurs were placed in the scanner with the long axis aligned to the axis of the scanner bed. The scanning parameters were as follows: pixel size 18 μm, tube voltage 50 kV, tube current 160 μA, aluminum filter 0.5 mm, 360° rotation angle with a rotation step of 1°. The SkyScan software package was used to reconstruct the image data and characterize the newly mineralized tissues. A cylindrical region of interest (ROI) 3 mm in diameter within the regenerating site was analyzed. The bone volume fraction and width of bone were estimated by bone volume per tissue volume (BV/TV) and trabecular thickness (Tb.Th), respectively.

2.7. Histological analysis and scores

After micro-CT scanning, the resected femurs were fixed for histological evaluation in 10% neutral-buffered formalin, dehydrated in graded alcohol, decalcified, sectioned perpendicular to the longitudinal axis in the center of repaired sites, and embedded in paraffin wax in accordance with standard processing in the Department of Pathology of Chi-Mei Medical Center. Tissue sections (4 μm thick) were stained with hematoxylin and eosin (H&E) for morphological evaluation and inflammatory responses, Masson's trichrome for general collagen accumulation and orientation, and Alcian blue for glycosaminoglycan (GAG) distribution. The specimens were observed under light microscopy (Olympus BX51, Japan) and recorded using a digital CCD camera (Olympus DP70, Japan). In addition, to further evaluate the specific contents of collagen type I (COL I, fibrocartilage), collagen type II (COL II, hyaline cartilage), collagen type X (COL X, hypertrophic or osteoarthritic cartilage), and cytokines such as TGF-β1 (chondrogenesis) as well as tumor necrosis factor-α (TNF-α) and interleukin-6 (IL-6) (inflammatory response and cartilage degeneration) in the reparative tissues, the sections were assessed by immunohistochemical (IHC) staining. The rabbit/mouse HRP/DAB polymer detection (BioTnA) kit was used. All primary antibodies were used in 1:100 dilutions. All staining protocols followed the suppliers' guidelines. The modified histological scores were quantitatively scored by two medical staff members according to the previous scoring system [25], providing a comprehensive evaluation of the cartilage and subchondral bone. For this study, the main categories of the histological scores comprise the overall filling assessment, subchondral morphology, bone filling, bonding to bone surface morphology, cartilage thickness, surface regularity, chondrocyte clustering, neosurface GAG and cell content, and adjacent surface GAG and cell

content. Moreover, the weighted scale was further highlighted with detailed percentage descriptions to differentiate the healing outcomes for hyaline-like cartilage and fibrocartilage, scored from 0 to 8 with an increment of 2, including mainly hyaline cartilage (>75%), hyaline cartilage mixed with fibrocartilage (50–75%), mainly fibrocartilage (>75%), mainly fibrous tissue (spherical cell morphology <75% of cells), and no tissue. Additionally, we evaluated the inflammation level based on the numbers of inflammatory cells (i.e., lymphocytes, plasma cells, or giant cells) and then scored from 0 to 3. The maximum score possible was 39 points (Table 1).

2.8. Statistical analysis

All data are shown as the mean ± standard error of the mean (SEM). Statistical analyses were performed using the SPSS v. 17.0 software package. Because of concerns about using repeated measurements from bilateral knees in the same individual [43], a linear model using generalized estimating equations (GEE) [44] was employed for statistical comparison at 6 and 12 weeks after surgery. Because the data were not normally distributed by the Shapiro–Wilk test and the homogeneity of variance was confirmed by the Levene's test, the nonparametric Mann–Whitney *U*-test was used to analyze the data for between-group comparisons. A significant difference was defined as a *p*-value <0.05.

3. Results

3.1. Rabbit health and exercise status

Of the 30 rabbits that were utilized in this study, all rabbits returned to their initial body weight over time after surgery. The general recovery time to functional activity with energetic actions and good appetite was observed within nearly 1 week. Skin wound closures healed by 12–14 days. None of the rabbits in the SED and TRE groups had signs of infection, joint swelling, or limited range of motion at 6 and 12 weeks after surgery. During the exercise program, rabbits had an even gait pattern and appeared to have no stress responses. The body temperature after exercise was significantly higher than that during the resting state (post-exercise: 40.73 ± 0.97 °C vs. resting: 35.9 ± 0.43 °C, *p* < 0.001), indicating a conditioning regulation.

3.2. Histological observations

3.2.1. Initiation of higher GAG, COL II, and TGF-β1 levels and of modest increases in COL I, COL X, inflammatory cells with TNF-α, and IL-6 in the PGI-TRE group

At week 6, the repaired joints in the TRE groups initiated more tissue coverage with visible chondroblasts and few chondrocytes in the defects, whereas the SED groups had disorganized and irregular surfaces, and the defect sites were covered with fibrous tissue containing fibroblast-like cells (Figs. 2A and 3A). In particular, the synovial-like lining cells migrating over the regenerating tissue were observed in the PGI-TRE group (Supplemental data 3). Overall, more chondroblasts had migrated into the center of the repaired tissue in the PGI groups than in the ED groups (Figs. 2A and 3A). With respect to inflammatory responses, the ED and PGI groups revealed the presence of plasma cells, lymphocytes, and multinucleated giant cells in the reparative sites (Fig. 2B). Particularly the ED-SED group manifested visible hemorrhage (Fig. 2B).

The PGI-TRE group had a modest inflammatory response, filled with more osteoid matrix, and appeared to form a vasculature (Figs. 2B and 3A). With respect to ECM synthesis, the PGI-TRE group had markedly higher levels of GAG in both neo-formed

Table 1
The histology scoring system.

	Category	Points
1. Percent filling with neo-formed tissue	75–100%	3
	50–75%	2
	25–50%	1
	0–25%	0
2. Percent filling with neo-formed tissue in subchondral bone	75–100%	3
	50–75%	2
	25–50%	1
	0–25%	0
3. Subchondral bone morphology	Normal, trabecular bone	4
	Trabecular, with some compact bone	3
	Compact bone	2
	Compact bone and fibrous tissue	1
	Only fibrous tissue or no tissue	0
4. Extent of neo-tissue bonding with adjacent bone in subchondral bone	Complete on both edges	3
	Complete on one edge	2
	Partial on both edges	1
	Without continuity on either edge	0
5. Morphology of neo-formed surface tissue	Mainly hyaline cartilage (>75%)	8
	Hyaline cartilage mixed with fibrocartilage (50–75%)	6
	Mainly Fibrocartilage (>75%)	4
	Mainly fibrous tissue (spherical cell morphology <75% of cells)	2
	No tissue	0
6. Thickness of neo-formed cartilage	Similar to the surrounding cartilage	3
	Greater than surrounding cartilage	2
	Less than the surrounding cartilage	1
	No cartilage	0
7. Joint surface regularity	Smooth, intact surface	3
	Surface fissures (<25% neo-surface thickness)	2
	Deep fissures (25–99% neo-surface thickness)	1
	Complete disruption of the neo-surface	0
8. Chondrocyte clustering	None at all	3
	Less than 25% of chondrocytes	2
	25–100% chondrocytes	1
	No chondrocytes present (no cartilage)	0
9. Chondrocyte and GAGs content of neo-cartilage	Normal cellularity with normal Alcian blue staining	3
	Normal cellularity with moderate Alcian blue staining	2
	Obviously less cells with poor Alcian blue staining	1
	Few cells with no or little Alcian blue staining or no cartilage	0
10. Chondrocyte and GAGs content of adjacent cartilage	Normal cellularity with normal Alcian blue staining	3
	Normal cellularity with moderate Alcian blue staining	2
	Obviously less cells with poor Alcian blue staining	1
	Few cells with no or little Alcian blue staining or no cartilage	0
11. Inflammatory response in the reparative site	Normal tissue (<5% inflammatory cells)	3
	Mild inflammation (5–20% inflammatory cells)	2
	Moderate inflammation (21–50% inflammatory cells)	1
	Severe (>50% inflammatory cells)	0
Total		39

tissue and adjacent cartilage (Fig. 3B) and clearly expressed both COL II and endogenous growth factor TGF-β1 as well as showing modest expression levels of COL I, COL X, TNF-α and IL-6 in the repaired region (Fig. 4). Nevertheless, the integration between hosts was distinct, and the PLGA grafts still remained clearly distinguishable (Figs. 2B and 3A). In contrast, the ED groups had little GAG in the neo-formed tissue and adjacent cartilage (Fig. 3B) and higher levels of COL I, COL X, TNF-α and IL-6 in addition to lower TGF-β1 expression (Fig. 4).

3.2.2. Development of hyaline cartilage and mature trabecular bone in the PGI-TRE group

At week 12, surprisingly, the PGI-TRE group demonstrated essentially original hyaline cartilage structures that appeared to have a sound chondrocyte orientation, a considerable level of GAG, and a high level of COL II (Figs. 2A, 3, and 4). Additionally,

inflammatory cells were minimally present in the defects, and COL I, COL X, TNF-α and IL-6 were observed to be modest (Figs. 2B and 4). Furthermore, the PGI-TRE group exhibited a smoother articulating surface and functionalized mature trabecular bone embedded with osteocytes in the integration sites (Figs. 2B and 3A). Furthermore, the tidemark was completely restored in the PGI-TRE group (Supplemental data 4). By contrast, the PGI-SED group exhibited fibrocartilaginous tissues containing little GAG that were mixed with irregular bone surrounding the defect (Fig. 3). The chondroblasts and dispersed chondrocytes were found in the chondral layer of the newly formed cartilage-like tissue (Fig. 2A), and the collagen fibers remained disorganized (Fig. 3A). In contrast, the knees in the ED-SED group remained concave with fibrous tissue in the defects, showed the destruction of the GAG from the host cartilage, included inflammatory cells as well as osteoclasts surrounding newly formed bone tissues (Figs. 2
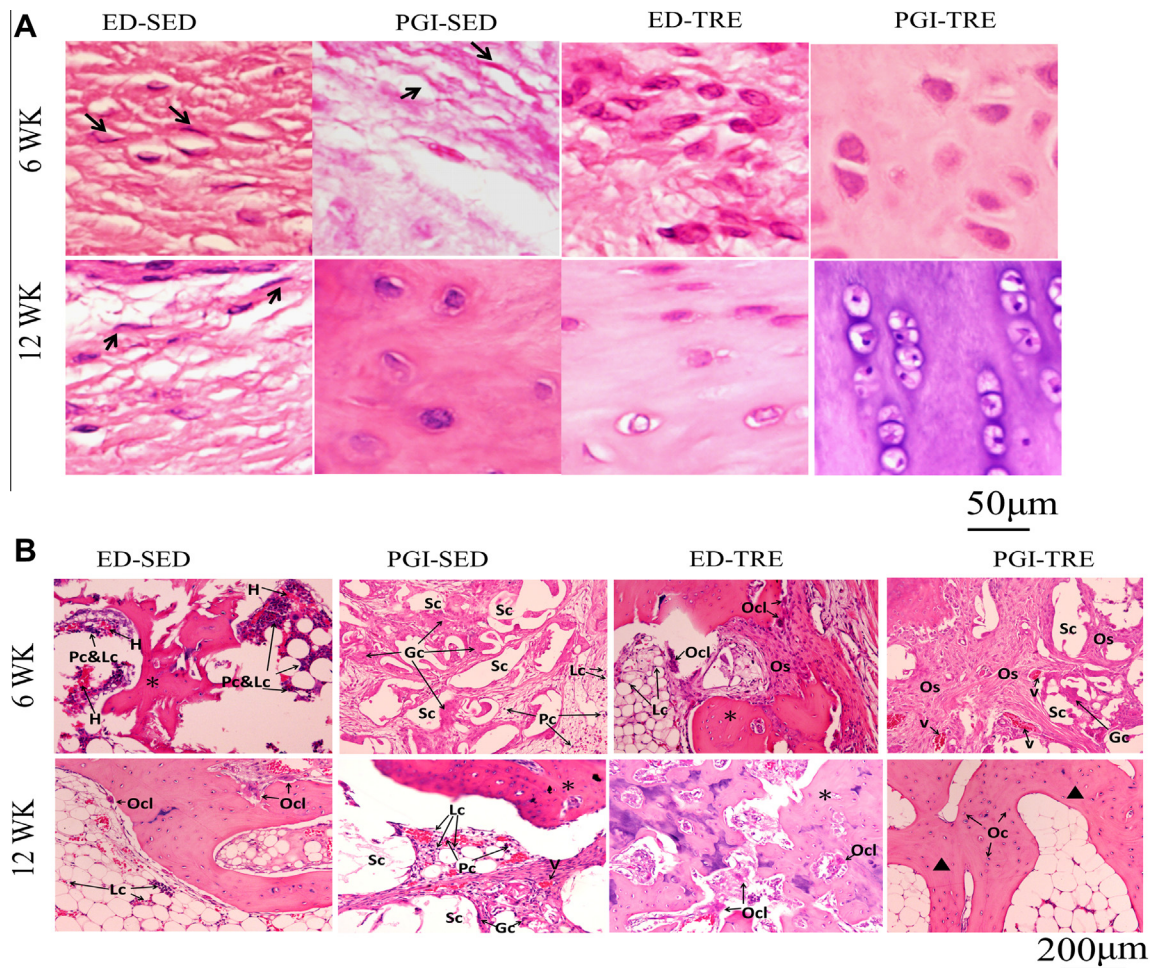
Fig. 2. (A) Observations of cell morphology in the chondral layer of the regenerative tissue. At week 6, the SED groups' defects were covered with fibrous tissue with fibroblast-like cells (arrow), whereas the TRE groups initiated more tissue coverage with visible chondroblasts and few chondrocytes in the defects. At week 12, the PGI-TRE group demonstrated essentially restored hyaline cartilage structures that appeared to have sound chondrocyte orientation as compared with other groups. (B) In subchondral reparative tissues, at week 6, the ED and PGI groups displayed inflammatory responses, including the representative presence of plasma cells (Pc), lymphocytes (Lc), and multinucleated giant cells (Gc). Particularly the ED-SED group manifested visible hemorrhage (H). In contrast, the PGI-TRE group had a modest inflammatory response, filled with more osteoid matrix (Os), and appeared to form a vasculature (v). At week 12, mild inflammatory cells such as Lc, and Pc, in addition to osteoclasts (Ocl), surrounding newly formed bone tissues were still shown in the ED and SED groups. Newly mineralized formation in the PGI-TRE group regenerated functionalized trabecular bone (▲) with embedded osteocytes (Oc), but the ED-TRE group showed predominantly compact bone (∗).

and 3), and is likely the enriched levels of COL I, COL X, TNF-α and IL-6 (Fig. 4). The ED-TRE group exhibited mainly fibrocartilage with little hyaline-like tissue and less GAG content in the repaired site but sustained the GAG content in the adjacent cartilage (Fig. 3).

3.3. Significantly higher histological scores in the PGI-TRE group

The histological scores are shown in Table 2. At week 6, the PGI-TRE group (23.71 ± 2.42) had significantly higher total scores than the ED-SED (15.83 ± 1.80, $p = 0.007$) and PGI-SED groups (17.40 ± 2.54, $p = 0.03$); at week 12, the PGI-TRE group (35.63 ± 1.07) showed significantly higher total scores than the ED-SED (18.17 ± 3.58, $p < 0.001$), PGI-SED (16.29 ± 2.16, $p < 0.001$) and ED-TRE (29.75 ± 2.17, $p = 0.027$) groups. In addition, the ED-TRE group at week 12 had significantly better scores than the ED-SED and PGI-SED groups. For comparisons of specific parameters, at week 12, the histological assessments in the PGI-TRE group revealed by far the best surface morphology (i.e., neo-formed hyaline cartilage), bone bonding, and GAG content. Moreover, with regard to inflammatory response, the PGI-TRE group showed a notably lower level of inflammation than the other groups at both 6 and 12 weeks.

3.4. Improvement of regenerating bone in the PGI-TRE group, as determined using μ-CT analysis

At week 6, newly synthesized mineral matrix regenerated from the border to the central hole of the defect region in all groups (Fig. 5A). The pattern of bone regeneration was noted to be top-to-bottom and edge-to-center, especially in the TRE groups (Fig. 5A). No apparent differences ($p > 0.05$) regarding BV/TV or Tb.Th values were observed in the ED groups, apart from the significantly higher BV/TV ($p = 0.036$) (Fig. 5C) and Tb.Th ($p < 0.001$) in the ED-TRE group (Fig. 5D). In addition, each treatment group showed significantly lower BV/TV and Tb.Th values ($p < 0.001$) than the sham group (Fig. 5C, D).

At week 12, the PGI groups showed more enhanced bony tissue at areas adjacent to the scaffolds than in the ED groups (Fig. 5A). Continuous architecture in regenerating sites was particularly observed in the PGI-TRE group (Fig. 5A, B). The ED-TRE group (37.58 ± 2.74) showed a significantly higher BV/TV than the ED-SED (26.30 ± 2.13) and PGI-SED (31.54 ± 3.10) groups ($p = 0.001$) (Fig. 5C), although an incomplete bridge was observed (Fig. 5A). In both the ED and PGI groups, significant Tb.Th was found in the TRE group relative to the SED group (Fig. 5D). Importantly, the
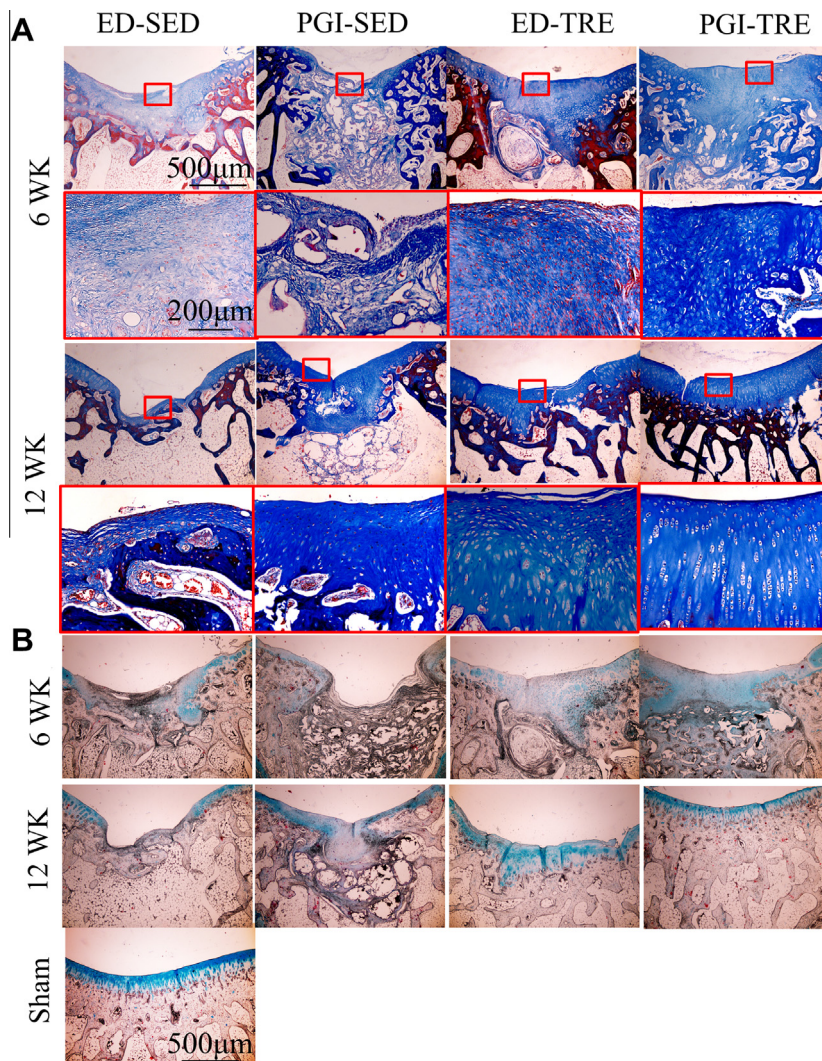
Fig. 3. Histological examinations using (A) Masson's trichrome and (B) Alcian blue staining. At week 6, the TRE groups manifested improved collagen alignment and content and higher GAG content, particularly in the PGI-TRE group. At week 12, the PGI-TRE group had the best regeneration outcomes, with the formation of hyaline-like cartilage and the development of columnar rounded chondrocytes with abundant GAG content. Squares denote the magnification scale. (For interpretation of the references to color in this figure legend, the reader is referred to the web version of this article.)

BV/TV in PCI-TRE group (44.70 ± 1.24) was significantly superior to the ED-TRE (37.58 ± 2.74) and PGI-SED (31.54 ± 3.10) groups ($p < 0.001$), with values similar to those observed for the sham group ($42.87.54 \pm 1.37$) (Fig. 5C).

4. Discussion

Cartilage regenerative medicine, including exogenous growth factors and scaffolds with or without cell fusion, has been adopted to remedy cartilaginous tissue, but few studies have considered the feasibility of repairing hyaline cartilage after graft implantation together with loading exercise during the early rehabilitation program. Accordingly, in the present study, we first implemented an implanted engineered cell-free porous PLGA graft along with treadmill exercise (i.e., the PGI-TRE group) that offered the stimulation of the in situ niche of the microenvironment for the remodeling of osteochondral defects. The PGI-TRE group showed significant improvement in the formation of neo-hyaline cartilage and the development of columnar rounded chondrocytes with enriched synthesis of COL II, GAG, and modest inflammation and cytokines (i.e., TNF-α, IL-6) as well as sound subchondral bone

formation (Figs. 2–5, Table 2). In contrast, the other groups in this rabbit model demonstrated incomplete cartilage regeneration. The cause of the observed success in the PCI-TRE group may be attributable to the following four critical components: a grafting substitute, a reasonable exercise program, mechanical stimuli in in-situ cells, and a substantially decreased inflammatory response in the reparative site.

Synthetic grafting substitutes can be fabricated using biodegradable and biocompatible materials and formed into porous scaffolds. Importantly, the grafting substitute plays a key role in subchondral bone remodeling. In this study, the one-layer spongy PLGA (lactide/glycolide ratio of 85/15) scaffold generates an affordable mechanical structure to bear the shear forces and loads encountered in the repaired region and also to bridge with the host to offer a space for in situ cell homing, attachment, and proliferation (Figs. 1A and 2A), where the synovial-like lining cells creates the chondrogenic potential (i.e., TGF-β1 cytokines) in the superficial regenerating defects (Fig. 4, Supplemental data 3). Moreover, regarding the osteochondral repair process, the functional survivability of articular cartilage may correspond to the subchondral bone repair (i.e., restoration of the tidemark), which offers a stable mechanical matrix and soundly integrated interface
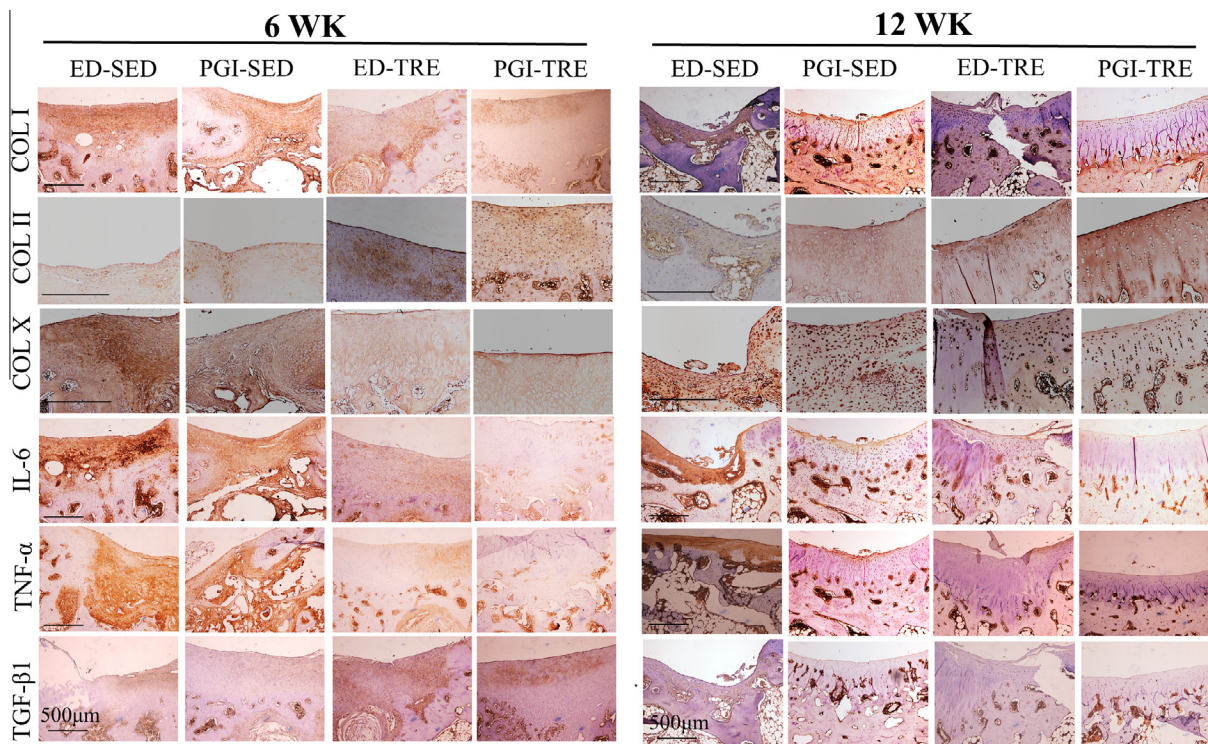
Fig. 4. Specific proteins and cytokines in the defect sites were detected by IHC staining. At week 6, the matrix in the PGI-TRE group expressed considerable amounts of COL II and TGF-β1, whereas the ED-SED group showed higher expression levels of COL I, COL X and inflammatory cytokines (i.e., TNF-α, IL-6). At week 12, the PGI-TRE group was rich in COL II, suggesting hyaline cartilage, and it showed modest levels of COL I, COL X and inflammatory cytokines (i.e., TNF-α, IL-6) compared with the other groups.

Table 2
Total histological scale scores. For each parameter, the values were expressed as the mean ± SEM.

	6 weeks				12 weeks			
	ED-SED	PGI-SED	ED-TRE	PGI-TRE	ED-SED	PGI-SED	ED-TRE	PGI-TRE
Overall filling	1.67 ± 0.21	2.60 ± 0.24	1.13 ± 0.33[b]	2.63 ± 0.26[a,c]	1.67 ± 0.21	1.71 ± 0.18	2.75 ± 0.25[a,b]	2.89 ± 0.11[a,b]
Bone filling	1.50 ± 0.22	2.20 ± 0.20	1.17 ± 0.31[b]	2.50 ± 0.27[a,c]	1.33 ± 0.21	1.43 ± 0.20	2.75 ± 0.25[a,b]	2.89 ± 0.11[a,b]
Subchondral morphology	2.33 ± 0.33	1.40 ± 0.51	1.33 ± 0.33	2.25 ± 0.37[c]	1.67 ± 0.61	1.29 ± 0.47	2.25 ± 0.25[b]	3.11 ± 0.31[b,c]
Bone bonding	1.00 ± 0.26	0.80 ± 0.80	1.00 ± 0.26	1.00 ± 0.19	1.67 ± 0.49	1.00 ± 0.44	2.00 ± 0.41[b]	2.44 ± 0.29[a,b,c]
Surface morphology	3.33 ± 0.42	3.20 ± 0.37	4.33 ± 0.61[b]	3.50 ± 0.63	3.67 ± 0.61	3.57 ± 0.75	6.00 ± 0.82[a,b]	7.11 ± 0.48[a,b,c]
Cartilage thickness	0.67 ± 0.21	0.80 ± 0.40	1.17 ± 0.31	1.00 ± 0.33	1.00 ± 0.37	1.29 ± 0.29	2.00 ± 0.41	2.56 ± 0.24[a,b]
Surface regularity	1.67 ± 0.21	1.60 ± 0.20	1.83 ± 0.40	1.88 ± 0.44	1.33 ± 0.49	1.86 ± 0.26	2.25 ± 0.48	2.67 ± 0.17[a,b,c]
Chondrocyte clustering	0.83 ± 0.17	1.20 ± 0.37	0.83 ± 0.17	1.00 ± 0.38	1.17 ± 0.40	1.43 ± 0.20	2.33 ± 0.25[a,b]	2.78 ± 0.15[a,b,c]
GAG&Cell content of neo-surface	0.67 ± 0.21	1.20 ± 0.37	1.67 ± 0.49	1.63 ± 0.26[a]	1.17 ± 0.31	1.43 ± 0.30	2.33 ± 0.29[a,b]	2.78 ± 0.15[a,b]
GAG&Cell content of adjacent surface	1.00 ± 0.00	1.20 ± 0.20	1.67 ± 0.21[a,b]	2.38 ± 0.18	1.83 ± 0.31	2.14 ± 0.26	2.50 ± 0.29[a,b]	2.89 ± 0.11[a,b]
Inflammation	1.17 ± 0.31	1.20 ± 0.37	1.33 ± 0.33	2.25 ± 0.16[a,b,c]	1.67 ± 0.21	1.29 ± 0.18	2.50 ± 0.29[a,b]	2.33 ± 0.17[a,b]
Total	15.83 ± 1.80	17.40 ± 2.54	20.40 ± 1.36	23.71 ± 2.42[a,b]	18.17 ± 3.58	16.29 ± 2.16	29.75 ± 2.17[a,b]	35.63 ± 1.07[a,b,c]

[a] Compared with the ED-SED group at the same time point ($p < 0.05$).
[b] Compared with the PGI-SED group at the same time point ($p < 0.05$).
[c] Compared to the ED-TRE group at the same time point ($p < 0.05$).

between the newly formed cartilage and the subchondral bone [45,46], as shown by the tidemark formation in this study (Supplemental data 4). In addition, the defect size in the current rabbit model was adopted such that the outcomes showed mainly fibrocartilage tissue or only fibrous tissue, indicating that any possibility of spontaneous recovery had been eliminated.

Proper loading exercises (i.e., mild to moderate intensity) in joints are essential to the regulation of cartilage turnover. The benefits include an increase in articular cartilage thickness and improvements in collagen formation, GAG density, and mineralized bone [47–49]. In contrast, intense exercise potentiates the harmful effects, such as a decrease in the mechanical properties of the cartilage, decline of GAG concentration, and osteoarthritic changes in subchondral bone [27]. In the present study, the exercise program included a total of 15 min/day, 5 days/week for

2 continuous weeks. The exercise intensity was adjusted to 1.0 km/hr, which is a mild to moderate exercise dosage for rabbits as described in a previous study [39], because New Zealand white rabbits have the capacity to run continuously on the treadmill for up to 21 min at 1.2 km/hr. As a result, adequate exercise benefits cartilage repair, indicating a sound articular surface, collagen and GAG contents (Figs. 3 and 4).

Mechanical stimulation actively drives the development of undifferentiating bone marrow-derived cells (BMCs) in the surrounding host and reparative sites. In the present study, cartilage could be regenerated by endogenous BMCs supplied from the drilled defect areas without any cell transplantation or additional exogenous growth factors. The timing of the loading exercise also plays a pivotal role in cartilage regeneration. Exercise initiated at 4 weeks after surgery generated a promising effect on the repair
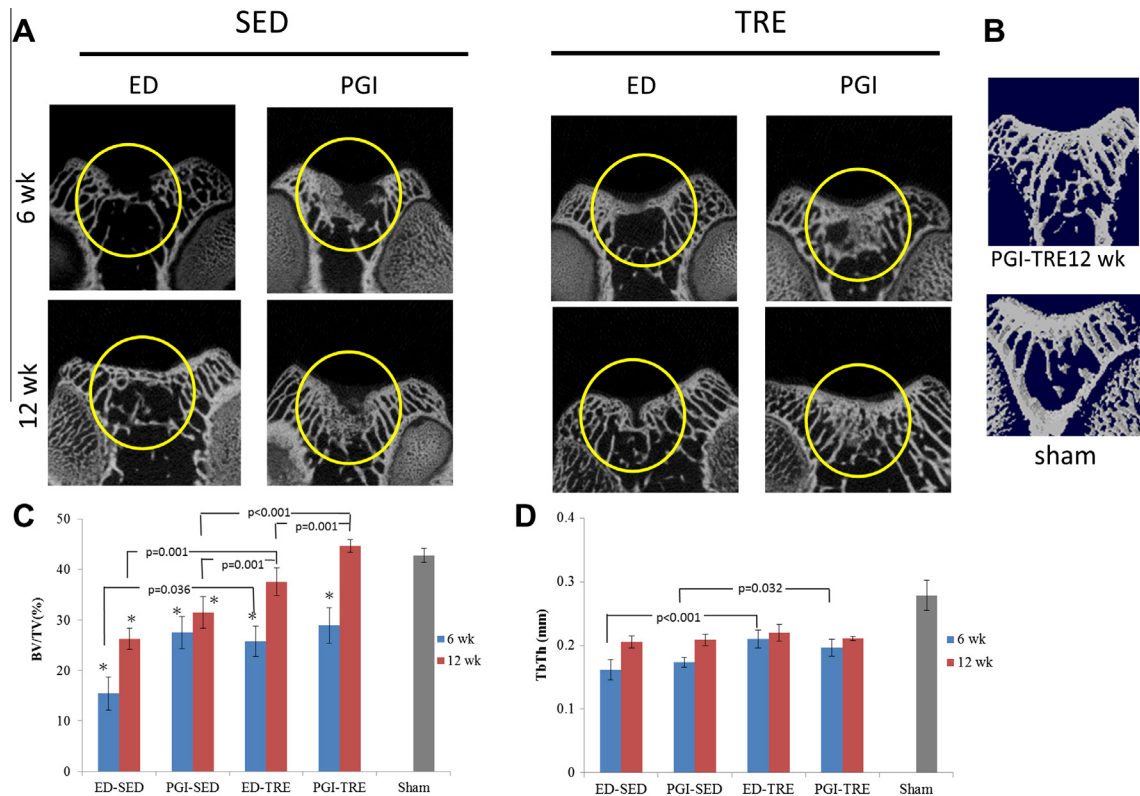
Fig. 5. (A) The bone assessment of 2D micro-CT images in the frontal plane; (B) 3D micro-CT images; (C) the ratio of bone volume to tissue volume (BV/TV); (D) the thickness of trabecular bone (Tb.Th).

of damaged cartilage (Figs. 2, 3, and 4A), consistent with a previous rat model [26]. It is possible that the newly formed matrix associated with active undifferentiated cells was appropriately filled with porous PLGA (Fig. 3). Cell–cell and cell–matrix interactions had been initiated by the perceived dynamic mechanical stimulation. Meanwhile, the main body of PLGA and the formed osteoid matrix served as a bridge in a net of loading transmission from the superficial chondral surface into the deep subchondral repair region during active knee flexion and extension movements. Eventually, a amount of organized collagen deposition, predominantly COL II, greater GAG synthesis in the regenerating cartilage, and sound subchondral bone formation were established in the PGI-TRE group (Figs. 3–5). Furthermore, functionalized trabecular bone embedded with mature osteocytes was regenerated (Fig. 2B). In contrast, the ED-TRE group exhibited mainly fibrocartilage with little hyaline-like tissue and less GAG in the repaired site (Fig. 3). From this perspective, loading exercise alone cannot be used as a major therapy for cartilage defects. However, it can be combined with the PLGA scaffold for cartilage repair in early rehabilitation. Still, loading exercise performed too early would collapse the host cartilage and damage the reparative site due to the unstable fundamental matrix structure; exercise begun too late would have no beneficial impact because the differentiated cells and structural ECM would have matured already [26].

Exercise directly exerts anti-inflammatory effects [6]; thus, the American College of Sports Medicine recently stated that "exercise is medicine". The synthesis and degradation of cartilage is determined by cytokines in the joint. The catabolic cytokines TNF-α and IL-6 act to decrease ECM synthesis during accelerated inflammation in joints, while the anabolic cytokines act to stimulate cartilage synthesis [6,50]. The anti-inflammatory effects of exercise be mediated via the sense of an anti-inflammatory microenvironment with each loading and unloading movement [51]. Conversely, physical inactivity increases the risk of inflammation [25]. In the

present study, the SED groups showed obvious elevation of the cytokines TNF-α and IL-6 (Fig. 4), which may be secreted by inflammatory cells (i.e., plasma cells, lymphocytes, and giant cells) and osteoclast activity (Fig. 2B); however, the TRE groups had modest TNF-α and IL-6 cytokine levels, indicating an anti-inflammatory response in the joint (Fig. 4).

Our study warrants further investigations in the future, including (1) experimental trials with specific models using larger defects of larger animal or human hosts with different loading regions, (2) scaling up the mechanical properties of the grafts implanted, and (3) performing positive technology transfer toward clinical good manufacturing practices (GMPs).

5. Conclusions

Our results suggest that it is feasible to remedy cartilage using a cell-free porous PLGA graft and hyaline cartilage regeneration and that an anti-inflammatory response can be further developed via early loading exercise for repairing osteochondral defects in the rabbit knee joint. This combined effect may pave the way for an alternative and advanced therapeutic strategy in cartilage regenerative medicine.

Appendix A. Supplementary data

Supplementary data associated with this article can be found, in the online version, at http://dx.doi.org/10.1016/j.actbio.2015.09.026.

References

[1] I.M. Khan, S.J. Gilbert, S.K. Singhrao, V.C. Duance, C.W. Archer, Cartilage integration: evaluation of the reasons for failure of integration during cartilage repair: A review, Eur. Cell Mater. 156 (2008) 26–39.

[2] S.E. Willick, P.A. Hansen, Running and osteoarthritis, Clin. Sports Med. 29 (2010) 417–428.

[3] M.B. Goldring, M. Otero, Inflammation in osteoarthritis, Curr. Opin. Rheumatol. 23 (2011) 471–478.

[4] J.D. Harris, R.A. Siston, X. Pan, D.C. Flanigan, Autologous chondrocyte implantation: a systematic review, J. Bone Joint Surg. Am. 92 (2010) 2220–2233.

[5] Y. Wang, L. Wei, L. Zeng, D. He, X. Wei, Nutrition and degeneration of articular cartilage, Knee Surg. Sports Traumatol. Arthrosc. 21 (2013) 1751–1762.

[6] M. Kapoor, J. Martel-Pelletier, D. Lajeunesse, J.P. Pelletier, H. Fahmi, Role of proinflammatory cytokines in the pathophysiology of osteoarthritis, Nat. Rev. Rheumatol. 7 (2011) 33–42.

[7] E. Kon, A. Roffi, G. Filardo, G. Tesei, M. Marcacci, Scaffold-based cartilage treatments: with or without cells? A systematic review of preclinical and clinical evidence, Arthroscopy 31 (2015) 767–775.

[8] J.A. Fazalare, M.J. Griesser, R.A. Siston, D.C. Flanigan, The use of continuous passive motion following knee cartilage defect surgery: a systematic review, Orthopedics 33 (2010) 878.

[9] N.J. Chang, Y.R. Jhung, C.K. Yao, M.L. Yeh, Hydrophilic gelatin and hyaluronic acid-treated PLGA scaffolds for cartilage tissue engineering, J. Appl. Biomater. Funct. Mater. 11 (2013) e45–e52.

[10] N.J. Chang, Y.R. Jhung, N. Issariyakul, C.K. Yao, M.L. Yeh, Synergistic stimuli by hydrodynamic pressure and hydrophilic coating on PLGA scaffolds for extracellular matrix synthesis of engineered cartilage, J. Biomater. Sci. Polym. Ed. 23 (17) (2012) 2133–2151.

[11] N.J. Chang, C.C. Lin, C.F. Li, K. Su, M.L. Yeh, The effect of osteochondral regeneration using polymer constructs and continuous passive motion therapy in the lower weight-bearing zone of femoral trocheal groove in rabbits, Ann. Biomed. Eng. 41 (2013) 385–397.

[12] N.J. Chang, C.F. Lam, C.C. Lin, W.L. Chen, C.F. Li, Y.T. Lin, M.L. Yeh, Transplantation of autologous endothelial progenitor cells in porous PLGA scaffolds create a microenvironment for the regeneration of hyaline cartilage in rabbits, Osteoarthritis Cartilage 21 (2013) 1613–1622.

[13] M. Camina, D. Peris, C. Fonseca, J. Barrachina, D. Codina, R.M. Rabanal, X. Moll, A. Morist, F. García, J.J. Cairó, F. Gòdia, A. Pla, J. Vives, Cartilage resurfacing potential of PLGA scaffolds loaded with autologous cells from cartilage, fat, and bone marrow in an ovine model of osteochondral focal defect, Cytotechnology (2015), http://dx.doi.org/10.1007/s10616-015-9842-4 [Epub ahead of print].

[14] W. Yang, S.K. Both, G.J. van Osch, Y. Wang, J.A. Jansen, F. Yang, Effects of in vitro chondrogenic priming time of bone-marrow-derived mesenchymal stromal cells on in vivo endochondral bone formation, Acta Biomater. 13 (2015) 254–265.

[15] Y. Qi, Y. Du, W. Li, X. Dai, T. Zhao, W. Yan, Cartilage repair using mesenchymal stem cell (MSC) sheet and MSCs-loaded bilayer PLGA scaffold in a rabbit model, Knee Surg. Sports Traumatol. Arthrosc. 21 (2014) 1424–1433.

[16] C. Fonseca, M. Caminal, D. Peris, J. Barrachina, P.J. Fabregas, F. Garcia, J.J. Cairó, F. Gòdia, A. Pla, J. Vives, An arthroscopic approach for the treatment of osteochondral focal defects with cell-free and cell-loaded PLGA scaffolds in sheep, Cytotechnology 66 (2014) 345–354.

[17] G.I. Im, H.J. Kim, J.H. Lee, Chondrogenesis of adipose stem cells in a porous PLGA scaffold impregnated with plasmid DNA containing SOX trio (SOX-5,-6 and -9) genes, Biomaterials 32 (2011) 4385–4392.

[18] H. Chiang, C.J. Liao, C.H. Hsieh, C.Y. Shen, Y.Y. Huang, C.C. Jiang, Clinical feasibility of a novel biphasic osteochondral composite for matrix-associated autologous chondrocyte implantation, Osteoarthritis Cartilage 21 (2013) 589–598.

[19] Q. Zhuo, W. Yang, J. Chen, Y. Wang, Metabolic syndrome meets osteoarthritis, Nat. Rev. Rheumatol. 8 (2012) 729–737.

[20] X. Gao, Q. Zhu, W. Gu, Analyzing the effects of mechanical and osmotic loading on glycosaminoglycan synthesis rate in cartilaginous tissues, J. Biomech. 48 (2015) 573–577.

[21] R.B. Salter, D.F. Simmonds, B.W. Malcolm, E.J. Rumble, D. MacMichael, N.D. Clements, The biological effect of continuous passive motion on the healing of full-thickness defects in articular cartilage. An experimental investigation in the rabbit, J. Bone Joint Surg. Am. 62 (1980) 1232–1251.

[22] L.A. Harvey, L. Brosseau, R.D. Herbert, Continuous passive motion following total knee arthroplasty in people with arthritis, Cochrane Database Syst. Rev. 2 (2014) CD004260.

[23] S.W. O'Driscoll, F.W. Keeley, R.B. Salter, Durability of regenerated articular cartilage produced by free autogenous periosteal grafts in major full-thickness defects in joint surfaces under the influence of continuous passive motion. A follow-up report at one year, J. Bone Joint Surg. Am. 70 (1988) 595–606.

[24] M.J. Palmoski, R.A. Colyer, K.D. Brand, Joint motion in the absence of normal loading does not maintain normal articular cartilage, Arthritis Rheum. 23 (1980) 325–334.

[25] N.J. Chang, C.C. Lin, C.F. Li, D.A. Wang, N. Issariyaku, M.L. Yeh, The combined effects of continuous passive motion treatment and acellular PLGA implants on osteochondral regeneration in the rabbit, Biomaterials 33 (2012) 3153–3163.

[26] J.Q. Song, F. Dong, X. Li, C.P. Xu, Z. Cui, N. Jiang, J.J. Jia, B. Yu, Effect of treadmill exercise timing on repair of full-thickness defects of articular cartilage by bone-derived mesenchymal stem cells: an experimental investigation in rats, PLoS ONE 9 (2014) e90858.

[27] G.X. Ni, S.Y. Liu, L. Lei, Z. Li, Y.Z. Zhou, L.Q. Zhan, Intensity-dependent effect of treadmill running on knee articular cartilage in a rat model, Biomed. Res. Int. 2013 (2013) 172392.

[28] D.C. Maldonado, M.C. Silva, R. Neto Sel, M.R. de Souza, R.R. de Souza, The effects of joint immobilization on articular cartilage of the knee in previously exercised rats, J. Anat. 222 (2013) 518–525.

[29] B. Vanwanseele, E. Lucchinetti, E. Stussi, The effects of immobilization on the characteristics of articular cartilage: current concepts and future directions, Osteoarthritis Cartilage 10 (2002) 408–419.

[30] K. Ren, C. He, C. Xiao, G. Li, X. Chen, Injectable glycopolypeptide hydrogels as biomimetic scaffolds for cartilage tissue engineering, Biomaterials 51 (2015) 238–249.

[31] C.R. Chu, M. Szczodry, S. Bruno, Animal models for cartilage regeneration and repair, Tissue Eng. Part B Rev. 16 (2010) 105–115.

[32] P. Julkunen, E.P. Halmesmäki, J. Iivarinen, L. Rieppo, T. Närhi, J. Marjanen, J. Rieppo, J. Arokoski, P.A. Brama, J.S. Jurvelin, H.J. Helminen, Effects of growth and exercise on composition, structural maturation and appearance of osteoarthritis in articular cartilage of hamsters, J. Anat. 217 (2010) 262–274.

[33] W. Kim, C.E. Kawcak, C.W. McIlwraith, E.C. Firth, B.H. McArdle, N.D. Broom, Influence of early conditioning exercise on the development of gross cartilage defects and swelling behavior of cartilage extracellular matrix in the equine midcarpal joint, Am. J. Vet. Res. 70 (2009) 589–598.

[34] P.R. van Weeren, E.C. Firth, H. Brommer, M.M. Hyttinen, A.E. Helminen, C.W. Rogers, J. Degroot, P.A. Brama, Early exercise advances the maturation of glycosaminoglycans and collagen in the extracellular matrix of articular cartilage in the horse, Equine Vet. J. 40 (2008) 128–135.

[35] S.A. Kincaid, D.C. Van Sickle, Effects of exercise on the histochemical changes of articular chondrocytes in adult dogs, Am. J. Vet. Res. 43 (1982) 1218–1226.

[36] P.E. Lammi, M.J. Lammi, R.H. Tammi, H.J. Helminen, M.M. Espanha, Strong hyaluronan expression in the full-thickness rat articular cartilage repair tissue, Histochem. Cell Biol. 115 (2001) 301–308.

[37] M.M. Espanha, P.E. Lammi, M.M. Hyttinen, M.J. Lammi, H.J. Helminen, Extracellular matrix composition of full-thickness defect repair tissue is little influenced by exercise in rat articular cartilage, Connect. Tissue Res. 42 (2001) 97–109.

[38] R.D. Howard, C.W. McIlwraith, G.W. Trotter, B.E. Powers, P.R. McFadden, F.L. Harwood, D. Amiel, Long-term fate and effects of exercise on sternal cartilage autografts used for repair of large osteochondral defects in horses, Am. J. Vet. Res. 55 (1994) 1158–1167.

[39] H. Meng, G.N. Pierce, Metabolic and physiological response of the rabbit to continuous and intermittent treadmill exercise, Can. J. Physiol. Pharmacol. 68 (1990) 856–862.

[40] H.J. Mankin, The reaction of articular cartilage to injury and osteoarthritis (first of two parts), N. Engl. J. Med. 291 (1974) 1285–1292.

[41] H.J. Kreder, M. Moran, F.W. Keeley, R.B. Salter, Biologic resurfacing of a major joint defect with cryopreserved allogeneic periosteum under the influence of continuous passive motion in a rabbit model, Clin. Orthop. Relat. Res. 300 (1994) 288–296.

[42] P.H. Chen, C.E. White, Comparison of rectal, microchip transponder, and infrared thermometry techniques for obtaining body temperature in the laboratory rabbit (Oryctolagus cuniculus), J. Am. Assoc. Lab. Anim. Sci. 45 (2006) 57–63.

[43] J. Ranstam, Repeated measurements, bilateral observations and pseudoreplicates, why does it matter?, Osteoarthritis Cartilage 20 (2012) 473–475

[44] J.A. Hanley, A. Negassa, M.D. Edwardes, J.E. Forrester, Statistical analysis of correlated data using generalized estimating equations: an orientation, Am. J. Epidemiol. 157 (2003) 364–375.

[45] C. Haasper, J. Zeichen, R. Meister, C. Krettek, M. Jagodzinski, Tissue engineering of osteochondral constructs in vitro using bioreactors, Injury 39 (2008) S66–S76.

[46] A. Boyde, The real response of bone to exercise, J. Anat. 203 (2003) 173–189.

[47] I. Kiviranta, M. Tammi, J. Jurvelin, A.M. Saamanen, H.J. Helminen, Moderate running exercise augments glycosaminoglycans and thickness of articular cartilage in the knee joint of young beagle dogs, J. Orthop. Res. 6 (1988) 188–195.

[48] G.X. Ni, L. Lei, Y.Z. Zhou, Intensity-dependent effect of treadmill running on lubricin metabolism of rat articular cartilage, Arthritis Res. Theor. 14 (2012) R256.

[49] H. Isaksson, V. Tolvanen, M.A. Finnila, J. Iivarinen, A. Turunen, T.S. Silvast, J. Tuukkanen, K. Seppänen, J.P. Arokoski, P.A. Brama, J.S. Jurvelin, H.J. Helminen, Long-term voluntary exercise of male mice induces more beneficial effects on cancellous and cortical bone than on the collagenous matrix, Exp. Gerontol. 44 (2009) 708–717.

[50] J.A. Roman-Blas, D.G. Stokes, S.A. Jimenez, Modulation of TGF-beta signaling by proinflammatory cytokines in articular chondrocytes, Osteoarthritis Cartilage 15 (2007) 1367–1377.

[51] D.M. Knapik, J.D. Harris, G. Pangrazzi, M.J. Griesser, R.A. Siston, S. Agarwal, D.C. Flanigan, The basic science of continuous passive motion in promoting knee health: a systematic review of studies in a rabbit model, Arthroscopy 29 (2013) 1722–1731.